

Title: Patterning solar cell metal grids on transparent conductive oxides using self-assembled phosphonic acid monolayers

Authors: Gaëlle A. L. Andreatta*, Agata Lachowicz, Nicolas Blondiaux, Christophe Allebé, Antonin Faes

Affiliation: Centre Suisse d'électronique et de Microtechnique CSEM, 1 rue Jaquet-Droz, CH-2002 Neuchâtel,

Switzerland

* Corresponding author

gaelle.andreatta@csem.ch

phone: +41 32 720 5681

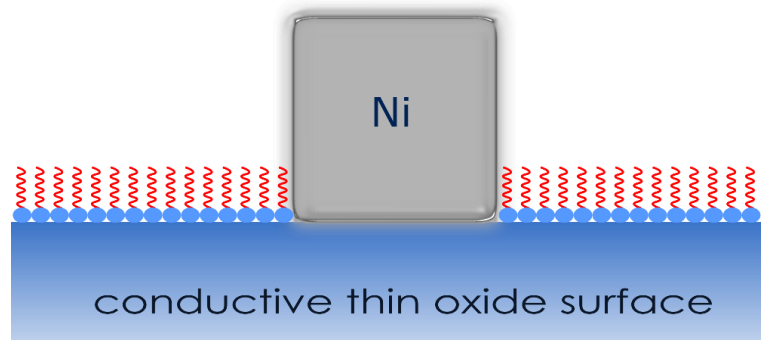
fax: +41 32 720 5750

Abstract:

We present a novel, simple and cost-effective method for patterning transparent conductive oxides (TCO) in order to form solar cell's metal grid by electro-plating. Self-assembled monolayers (SAMs) are prepared by dipping substrates in or spraying TCO with perfluorinated and alkylated phosphonic acid solutions. The investigated chemistry and explored deposition parameters on Indium Tin Oxide (ITO) have resulted in highly hydrophobic surfaces with exceptional coverage of the TCO by the SAMs. The resistance of the deposited layers to acidic plating conditions has been a challenge but layers at optimized processing conditions have demonstrated masking properties for nickel electroplating.

Keywords: self-assembled monolayers, phosphonic acid, transparent conductive oxide, indium tin oxide, electroplating, silicon heterojunction solar cells

Graphical abstract



Highlights:

- Dense, self-assembled monolayers of phosphonic acids on indium tin oxide surfaces of silicon heterojunction solar cells are produced by a simple and cost-effective spraying method.
- Good chemical resistance to highly acidic copper electrolyte is provided by the self-assembled monolayer and low degradation of ITO is observed after 10 minute immersion in solutions of $\text{pH} < 1$.
- Thin nickel lines are obtained on a patterned self-assembled monolayer on ITO by electroplating with little ghost-plating.

1. Introduction

At the time silicon-based homojunction solar cells still dominate the solar industry, silicon hetero-junction (HJT) solar cells have the intrinsic qualities to overthrow it: low surface recombination losses, high operating voltages, simple structure with low manufacturing cost potential, low temperature and a native bifaciality [1]. The conductor grids for HJT cells are typically made of screen-printed silver paste with significant costs compared to standard homojunction solar cells. To prevent silicon passivation damages, curing temperature is limited to value below 250°C. However this low curing temperature causes a higher resistivity of the paste compared to standard firing through ones. [2,3].

Being a highly conductive material and hundred times cheaper than silver, copper is a promising candidate to boost solar cell efficiency while reducing material costs. Copper plating is thus seen as an interesting alternative to screen-printed silver. The technological challenges for plating on HJT cells consist in first reaching precise and affordable TCO patterning, then demonstrating a high adhesion of copper grid onto the cell TCO with a low contact resistance, high line conductance and minimum shading (< 30 μm line width). We have previously developed advanced processes for patterning and electroplating of copper, yielding demonstration of high performance solar cells, qualified with 24.7% certified efficiency for a cell with busbars [4,5]. The process of record is based on a patterning approach using a PVD seed layer deposited on the full wafer surface combined with inkjet printing of a hotmelt mask and etch-back processes.

We propose here a novel concept based on self-assembled monolayers (SAMs) in order to obtain patterned copper lines on TCOs. Since SAMs utilize an extremely small amount of material, this approach could achieve plating selectivity with ultra-low costs. Breen *et al.* described previously the use of microcontact printing and wet etching to pattern films of the transparent conductors indium tin oxide (ITO) and indium zinc oxide (IZO) [6]. Luscombe *et al.* used perfluorinated

silane SAMs deposited on ITO via compressed carbon dioxide, patterned by e-beam, as etch-resist to produce electrodes [7]. In both cases, a low concentration solution of oxalic acid is used to etch the TCOs, and the patterning methods are difficult to scale up at low costs. It was also shown that SAMs of phosphonic acid derivatives could act effectively as anticorrosion layers on metals [8]. She et al. reported the use of self-assembled monolayers of thiols on gold as template for electrodeposition of gold or copper [9,10]. We report here the formation of SAMs of long-chained phosphonic acids and their resistance to very low pH copper electrolyte. We also present preliminary results of the application of SAM layers as a patterned resist to plate thin lines of nickel, nickel here being meant to become an adhesion layer prior to copper plating.

2. Materials and methods

2.1 Materials

12,12,13,13,14,14,15,15,15,15-nonafluoropentadecylphosphonic acid (fC15-PA), 12,12,13,13,14,14,15,15,16,16,17,17-tridecafluoroseptadecylphosphonic acid (fC17-PA), 12,12,13,13,14,14,15,15,16,16,17,17,18,18,19,19,19-Heptadecafluorononadecylphosphonic acid (fC19-PA), and 10,11-Bis(2,2,3,3,4,4,5,5,6,6,7,7,8,8,9,9-Heptadecafluorononyl)icosane-1,20-diyl diphosphonic acid (bis-fC19-bisPA) were purchased from Sikemia and used as received. Chemical formulas are shown in Figure 1. Octadecylphosphonic acid (C18-PA) was purchased from Sigma-Aldrich and used as received. Ethanol (VLSI grade) was purchased from KMG Ultra Pure Chemicals SAS (France) and used as received.

Nickel electrolyte Ni-sulphamate HS from Atotech GmbH was used for plating tests.

Flat substrates were prepared by depositing 115 nm ITO by sputtering from a target with composition 90/10 indium oxide/tin oxide by weight using an Indeotec Octopus II sputtering tool on single side polished silicon wafers. The wafers were supplied by Si-Mat, Germany.

Structured substrates were heterojunction cell precursors made of pyramid-textured n-type monocrystalline silicon wafers with amorphous Si layers and ITO on both sides. The thickness of ITO measured on the glass reference is 115 nm. The thickness on a textured substrate is calculated to be 68 nm. The solar cells precursors were provided by CEA INES.

2.2 Self-assembled monolayers deposition

After cleaning and activating the TCO surface by an oxygen plasma (PlasmaLab 80+, Oxford instruments, power: 100W, pressure: 200mTorr, Flow: 50sccm O₂), the samples were either immersed in or sprayed by a solution of 5 mM phosphonic acid in ethanol. The spray-coating was performed at room temperature using a Nordson spray head attached to a Janome dosing system. Immersion was done at 70°C during one hour. The excess material was rinsed off with ethanol, dried with nitrogen flow and the samples were cured in a low-vacuum oven at 120°C.

2.3 Wettability measurements

The wettability changes of the surfaces were characterized by measuring the contact angle of water sessile droplets deposited on the sample. Advancing and receding water contact angles were determined using a Drop Shape Analysis System DSA30 provided by Krüss (Hamburg, Germany). Standard deviations were calculated using three measurements and the error bars shown on the graphs correspond to the 95% confidence intervals.

2.4 Electrolyte immersion tests

A highly acidic, electrolyte solution of 200 g/L of copper sulfate pentahydrate (corresponding to 50 g/L copper ions) and 50 g/L sulfuric acid in water was used to assess the stability of the phosphonic acid self-assembled monolayers. SAMs covered samples were partially immersed in a commercial copper electrolyte ($\text{pH} < 1$) during 10 minutes, rinsed in water and dried. The samples were characterized before and after immersion by optical microscopy and contact angle measurements

2.5 Patterning method

SAMs covered samples were patterned by covering with a silicon hard mask comprising thin lines of different width, placing the sample for 30 s in a RIE oxygen plasma (PlasmaLab 80+, Oxford Instruments). The removal of the SAMs was observed by checking the wettability patterns on the surface. The parts exposed to the plasma were wetting water, while the parts covered by the mask retained their hydrophobicity.

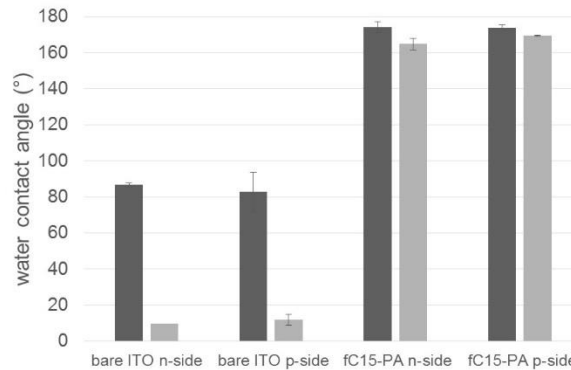
2.6 Electroplating tests and characterization.

Plating test were conducted in a small laboratory setup with 0.5 liter Nickel electrolyte, Ni-sulphamate HS at 45°C. The pH of the electrolyte was 4.4. The samples were textured heterojunction precursors covered with SAMs on both sides and cut in to pieces of 5 cm x 5 cm. For contacting the SAMs coating has been removed on one edge of the sample by dipping in concentrated sulfuric acid. The sample has been the contacted for plating with a conductive copper tape directly on the TCO. The samples have been plated at low current density, 1.5 A/dm² for 5 minutes and evaluated visually and by confocal microscope for plating selectivity or parasitic plating on SAM coated area (ghost-plating) respectively.

3. Results and discussion

3.1 Wettability and effect on the resistance to highly acidic electrolytes

We first measured the advancing and receding water contact angles on pyramid-textured solar cell precursors coated with intrinsic and doped hydrogenated amorphous silicon (a-Si:H) and



ITO on both sides(n-side and p-side).

Figure 2 shows the effect of covering the surface with a SAM prepared with fC15-PA. Due to the high roughness of the surface, the droplets of water are in so-called Wenzel state prior to the SAM spraying as shown by the large hysteresis between advancing and receding water contact angle [11,12]. Once covered with the SAM, the water droplets are in Cassie Baxter state [13]. The surface becomes superhydrophobic with advancing and receding well over 160°. Moreover a very low contact angle hysteresis was observed, thus attesting the high coverage of the surface by the SAM. The effect of the cell polarity on the measured contact angles appears to be minimal, as expected since the ITO surface is the same on both sides.

The advancing and receding water contact angles were also measured after immersing a sample in a highly acidic copper electrolyte solution for 10 minutes, which is equivalent to the time that would be used during copper electroplating. The results are shown in Figure 3. The superhydrophobicity was not affected by the immersion in the electrolyte. To separate the effect

of the surface chemistry and the high roughness of the functional substrates, ITO covered silicon wafers with very low roughness were prepared for all other measurements in this section.

SAMs were prepared with the perfluorinated phosphonic acids described in Figure 1 as well as octadecyl phosphonic acid (C18-PA) on low roughness ITO. Dynamic contact angles were measured before and after 10 minutes immersion in a highly acidic copper electrolyte. The results are shown in Figure 4. From these data, we can infer that the ITO is not well protected for that amount of time by the fC15-PA, f17-PA, f19-PA, but partially protected by the bis-f19-bis-PA and C18-PA. It is likely that the latter molecules are more organized at the interface.

Fluorocarbon chains are known to cause disruption in inter-chain packing [14]. While hydrocarbon chains present a linear structure, perfluorinated chains form helical structure and therefore self-assemble in less compact and more disordered layers [15].

Observations of the surface after immersion also confirm a lesser attack of the ITO surface when covered by bis-f19-bis-PA and C18-PA molecules. The results are shown in Figure 5. When the surface was not exposed, a smooth white image is observed on the optical microscope. However, in the parts that were immersed, especially on the samples covered by fC15-PA and fC17-PA, the ITO was visibly attacked and etched by the solution and a blue background is observed.

Various patterns are also observed. From these images, it is clear that while there is an improvement in the protection granted by the longer fC19-PA, the C18-PA and bis-fC19-bis-PA provide the best protection against corrosion by the highly acidic copper electrolyte. We interpret this as a result of a better packing of the hydrophobic chains in the self-assembled monolayers.

3.2 Preliminary results of nickel plating tests on patterned self-assembled monolayers

The process flow for production of HJT solar cells requires a first layer of nickel to be electroplated on the TCO in order to provide sufficient adhesion for the copper lines. Results discussed presently correspond to nickel plating tests. Figure 6 shows the patterned nickel lines obtained in a mild (pH=4.4) sulphamate nickel electroplating bath. The tests were done on f-C15-PA SAMs with and without patterning by removing the SAM using oxygen plasma combined with a hard mask. Prior to the electroplating step, one sample edge is dipped in concentrated sulfuric acid to remove the SAM and to allow contacting.

The unpatterned sample shows that the plating is selective and the SAM works as a resist. On the patterned samples, nickel lines are well defined and the plating limit shows little blurring (Figure 7). Depending on the length of time of the plasma patterning step, either 15 s or 30 s, the thinnest conductive line observed varies in width and length. For 15 s removal time, we measured a width of the thinnest line of 62.5 μm and height of 2.5 μm , while for 30s removal time, the measured width of the thinnest line is 82.1 μm and the height 3.6 μm . Therefore the nanolayer formed by the perfluorinated phosphonic acid molecules allows the electroplating of μm -high Ni lines. However the patterning has not been optimized. These first tests were done with a simple home-made mask produced by laser engraving silicon wafers. The patterning is still under development. We also plan to test laser patterning of the SAM.

In this process, the extremely low amount of material including solvents used for the SAM spraying makes our process cost-effective and eco-friendly.

However some ghost-plating is observed on the surface where the SAM remained after the plasma treatment. We plan to improve this by strengthening the organization of the SAM using the C18-PA and bis-C19-bis-PA molecules described in section 3.1. Some small nickel dots are also observed in places as shown on Figure 6. We assume that the SAM may have been damaged

by the contact with the hard-mask on the top of the microstructures of the substrates. It has been noticed (data not shown here) that the SAM is very sensitive to handling and might be easily rubbed off. In order to increase the plating quality, we will also investigated modifications of the patterning method to avoid damaging the SAM.

4. Conclusions

A spraying method was developed to produce perfluorinated and alkyl phosphonic acids self-assembled monolayers on pyramid-textured and polished silicon coated with indium tin oxide (ITO) surfaces. On textured substrates, superhydrophobic behavior was observed. The dynamic water contact angle measurements show very small hysteresis between the advancing and receding contact angles. This demonstrate the high quality of the self-assembly of molecules on the surface. We showed that the self-assembled monolayer provide ITO with a resistance to highly acidic electrolytes electroplating solutions. We are thus able to use the SAM as a resist for electroplating nickel. The layer of phosphonic acids can be patterned by a RIE oxygen plasma combined with a silicon hard mask. We have obtained well-defined, μm -thick conductive nickel lines by electroplating on the ITO substrate. We plan to improve the quality of the SAMs, patterning and to use to SAMs for copper electroplating in the future.

5. Acknowledgements

This work was supported by the Swiss National Science Foundation (SNF) and Agence Nationale de la Recherche (ANR). The authors thank CEA-INES (France) for providing the

microstructured solar cells precursors, Dr Jonas Geissbühler for the patterned silicon hard mask and Dr Gabriel Christmann for the deposition of ITO onto single side polished silicon wafers.

6. Bibliography

- [1] A. Descoeurdes, C. Allebé, N. Badel, L. Barraud, J. Champlaud, G. Christmann, F. Debrot, A. Faes, J. Geissbühler, J. Horzel, A. Lachowicz, J. Levrat, S.M. De Nicolas, S. Nicolay, L. Senaud, C. Ballif, M. Despeisse, Low-temperature processes for passivation and metallization of high- efficiency crystalline silicon solar cells, *Sol. Energy*. 175 (2018) 54–59. doi:10.1016/j.solener.2018.01.074.
- [2] J. Lossen, M. Matusovsky, A. Noy, C. Maier, M. Bähr, Pattern Transfer Printing (PTPTM) for c-Si Solar Cell Metallization, *Energy Procedia*. 67 (2015) 156–162. doi:10.1016/j.egypro.2015.03.299.
- [3] A. Faes, A. Lachowicz, A. Bettinelli, P. Ribeyron, J. Lerat, D. Munoz, J. Geissbühler, H. Li, C. Ballif, M. Despeisse, Metallization and interconnection for high-efficiency bifacial silicon heterojunction solar cells and modules, (2017).
- [4] A. Lachowicz, J. Geissbühler, A. Faes, J. Champlaud, F. Debrot, E. Kobayashi, J. Horzel, C. Ballif, M. Despeisse, Copper plating process for bifacial heterojunction solar cells, in: *Proc. 33rd Eur. Photovolt. Sol. Energy Conf. Exhib.*, 2017: pp. 1–4.
- [5] A. Lachowicz, P. Wyss, J. Geissbühler, A. Faes, J. Champlaud, N. Badel, C. Ballif, M. Despeisse, Review on plating processes for silicon heterojunction solar cells, 8th Work. Met. Interconnect. Cryst. Silicon Sol. Cells. (2019). http://www.metallizationworkshop.info/fileadmin/metallizationworkshop/presentations2019/5.2_Lachowicz_20190530_MIW_ReviewCuPlatingHJTCells.pdf (accessed June 20, 2019).
- [6] T.L. Breen, P.M. Fryer, R.W. Nunes, M.E. Rothwell, Patterning Indium Tin Oxide and Indium Zinc Oxide Using Microcontact Printing and Wet Etching, *Langmuir*. 18 (2002) 194–197. doi:https://doi.org/10.1021/la015543g.
- [7] C.K. Luscombe, H. Li, W.T.S. Huck, A.B. Holmes, Fluorinated Silane Self-Assembled Monolayers as Resists for Patterning Indium Tin Oxide, *Langmuir*. 19 (2003) 5273–5278.

- [8] T. Abohalkuma, F. Shawish, J. Telegdi, Phosphonic acid derivatives used in self assembled layers against metal corrosion, *Int. J. Corros. Scale Inhib.* 3 (2014) 151–159. doi:10.17675/2305-6894-2014-3-3-151-159.
- [9] Z. She, A. Difalco, G. Hähner, M. Buck, Electron-beam patterned self-assembled monolayers as templates for Cu electrodeposition and lift-off, *Beilstein J. Nanotechnol.* 3 (2012) 101–113. doi:10.3762/bjnano.3.11.
- [10] Z. She, A. Difalco, G. Hähner, M. Buck, Electrodeposition of gold templated by patterned thiol monolayers, *Appl. Surf. Sci.* 373 (2016) 51–60. doi:10.1016/j.apsusc.2015.12.054.
- [11] R.N. Wenzel, Resistance of solid surfaces to wetting by water., *Ind. Eng. Chem.* 28 (1936) 988–994.
- [12] A. Lafuma, D. Quéré, Superhydrophobic states, *Nat. Mater.* 2 (2003) 457–460. doi:10.1038/nmat924.
- [13] A.B.D. Cassie, S. Baxter, Wettability of Porous Surfaces, *Trans. Faraday Soc.* 40 (1944) 546–551. doi:10.1039/TF94444000546.
- [14] P. Chinwangso, L.R. St Hill, M.D. Marquez, T.R. Lee, Unsymmetrical Spiroalkanedithiols Having Mixed Fluorinated and Alkyl Tailgroups of Varying Length : Film Structure and Interfacial Properties, *Molecules.* 23 (2018) 2632. doi:10.3390/molecules23102632.
- [15] O.P. Khatri, D. Devaprakasam, S.K. Biswas, Frictional Responses of Octadecyltrichlorosilane (OTS) and 1H, 1H, 2H, 2H-Perfluorooctyltrichlorosilane (FOTS) Monolayers Self-assembled on Aluminium over Six Orders of Contact Length Scale, *Tribol. Lett.* 20 (2005) 235–246. doi:https://doi.org/10.1007/s11249-005-8551-0.

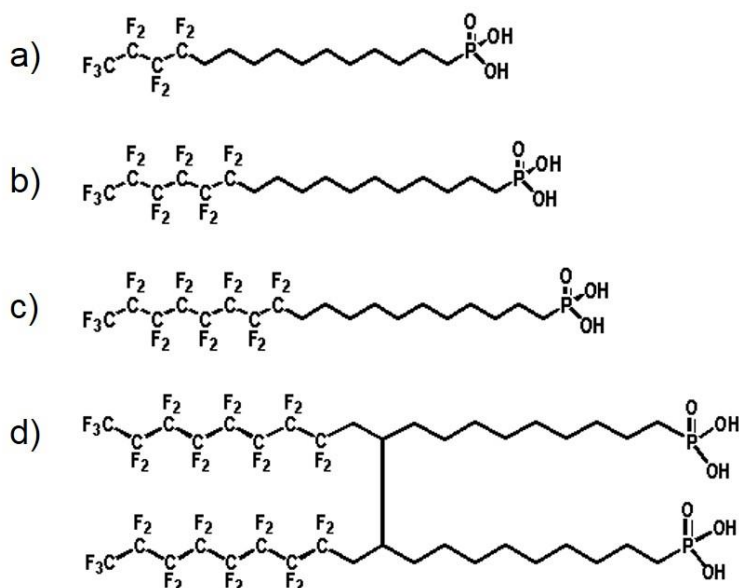


Figure 1: chemical formulas of all perfluorinated phosphonic acids used in this work. a) 12,12,13,13,14,14,15,15,15,15-nonafluoropentadecylphosphonic acid (fC15-PA), b) 12,12,13,13,14,14,15,15,16,16,17,17,17-tridecafluoroseptadecylphosphonic acid (fC17-PA), c) 12,12,13,13,14,14,15,15,16,16,17,17,18,18,19,19,19-Heptadecafluorononadecylphosphonic acid (fC19-PA), and d) 10,11-Bis(2,2,3,3,4,4,5,5,6,6,7,7,8,8,9,9,9-Heptadecafluorononyl)icosane-1,20-diyl diphosphonic acid (bis-fC19-bisPA).

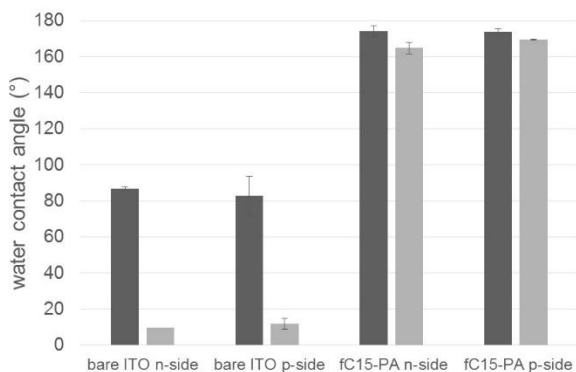


Figure 2: Water contact angles on structured ITO surfaces with different doping (n- and p-types) before and after applying the perfluorinated phosphonic acid SAM. The advancing contact angle is in dark grey and the receding in light grey.

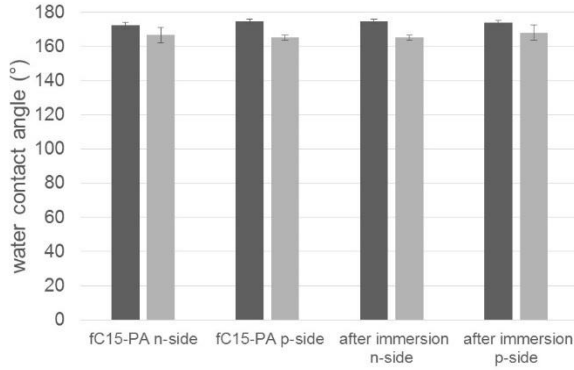


Figure 3: Water contact angles on fC15-PA covered ITO microstructured substrates with different doping (n- and p-types) before and after immersing the SAM in highly acidic copper electrolyte. The advancing contact angle is in dark grey and the receding in light grey.

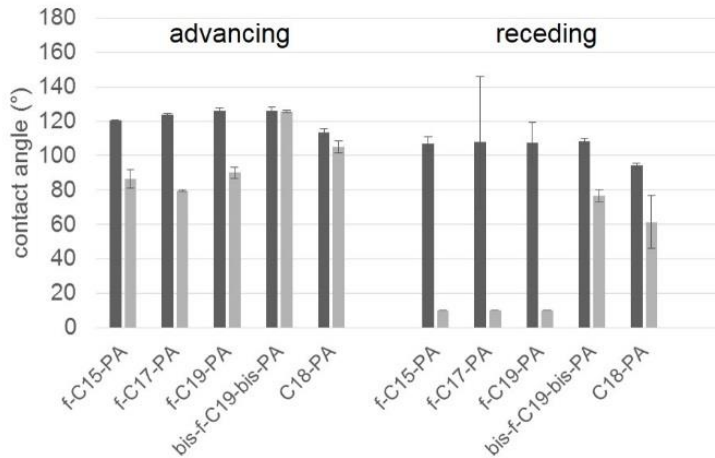


Figure 4: Dynamic water contact angles of various SAMs on very low roughness ITO surface. The contact angles were taken before (dark grey) and after immersion (light grey bars) during 10 min in highly acidic copper electrolyte. When the measured value of the receding contact angle was $<10^\circ$, it was deemed unreliable and arbitrarily replaced by the value of 10° .

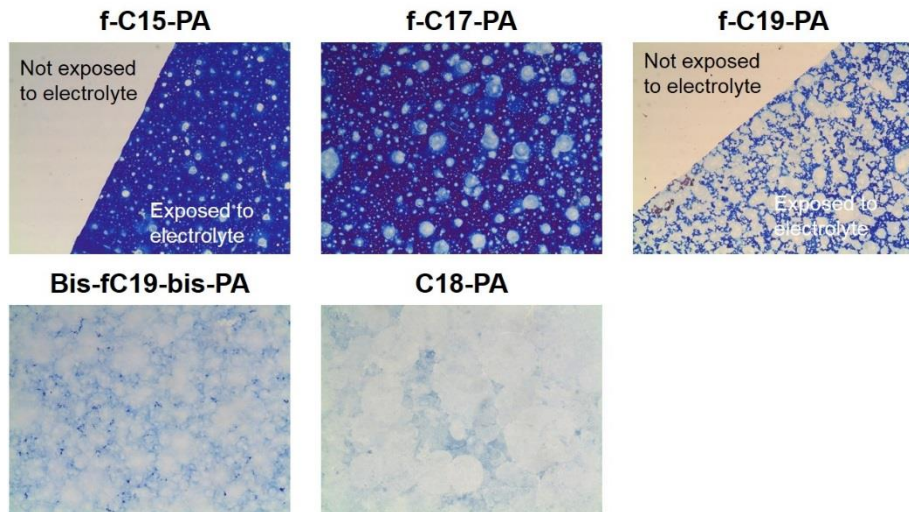


Figure 5: optical microscope images taken with a 5x objective after exposure to a copper electrolyte solution at very low pH (<1) during 10 minutes. When the surface was not exposed, a smooth white image is observed. When the ITO was visibly attacked and etched by the solution, a blue image is observed. Microstructures are also observed.

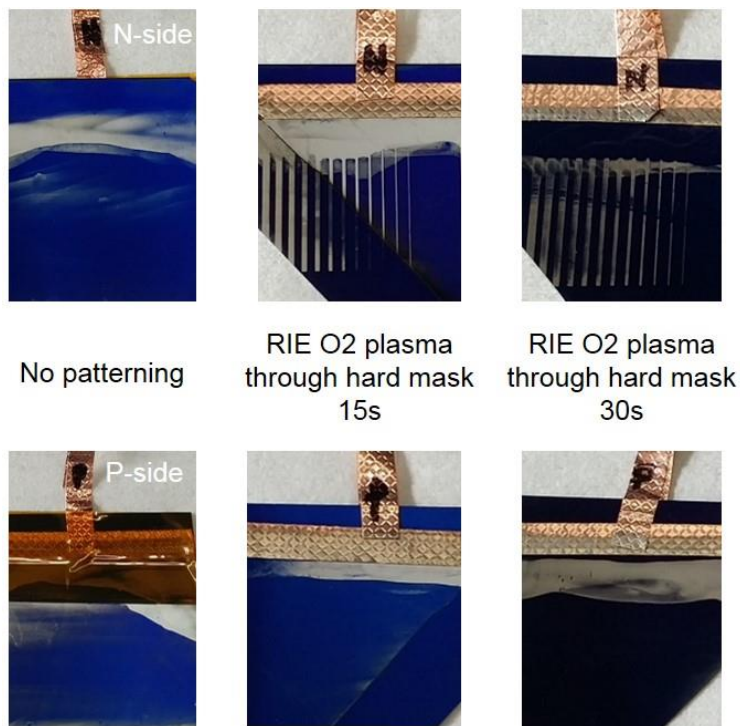


Figure 6: Pictures of three samples after nickel electroplating on the n-side (top) and p-side (bottom) using a fC15-PA SAM as resist. The top of each sample was dipped in a sulfuric acid solution to partially remove the SAM in order to make a contact. From left to right: 1. unpatterned sample placed in plating solution. Some ghost-plating is observed mostly on the p-side of the sample. 2. Sample patterned on the n-side using a silicon hard mask by a directional RIE O₂ plasma during 15s. Well defined plating lines are observed as well as some residual ghost-plating. Unfortunately the sample broke during the plating. 3. Sample patterned on the n-

side using a silicon hard mask by a directional RIE O₂ plasma during 30s. Well defined plating lines are observed as well as some residual ghost-plating. Unfortunately the sample broke during the plating.

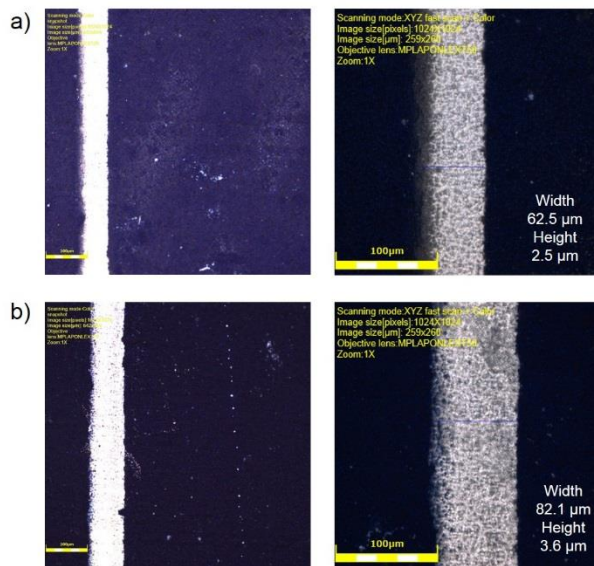


Figure 7: scanning confocal microscopy images taken on samples shown in Figure 6. a) images taken on the thinnest line of the sample patterned during 15s. Ghost-plating is evidenced on some of the masked parts. b) images taken on the thinnest line of the sample patterned during 30s. Some of the phosphonic acid layer may have been damaged by the hard mask as evidenced by the white dots on the masked part.